UNIVERSITÀ
DEGLI STUDI
DI UDINE

Università degli studi di Udine

Rotational effects on the flow field inside a leading edge impingement cooling passage

Original

Availability:
This version is available http://hdl.handle.net/11390/1088905 since 2020-02-20T16:54:32Z

Publisher:

Published
DOI:10.1016/j.expthermflusci.2016.03.004

Terms of use:
The institutional repository of the University of Udine (http://air.uniud.it) is provided by ARIC services. The aim is to enable open access to all the world.

Publisher copyright

(Article begins on next page)

14 May 2024

Rotational Effects on the Flow Field inside a Leading Edge Impingement Cooling Passage

Luca Furlani, Alessandro Armellini, Luca Casarsa
Dipartimento Politecnico di Ingegneria e Architettura, Università degli Studi di Udine
via delle Scienze 206, Udine, Italy

Abstract

The work reports for the first time detailed experimental data about the flow field inside an advanced leading edge cooling channel for gas turbine blades. The geometry key features are multiple internal impinging jests and coolant extraction for blade film cooling protection. Measurements have been performed by means of 2D and Stereo PIV, in both static and rotating conditions, with Reynolds number of 30k and 10k and a Rotation number of 0.05, both defined with reference to the jet characteristics. Different crossflow conditions in the feeding channel have been used to simulate the three main blade regions (i.e. HUB, MID, and TIP).
The flow inside the feeding channel is significantly affected by rotation, conversely, when moving inside the main impingement duct, the jet core has been found to be only marginal modified due to rotation. Finally, a substantial Reynolds number independence has been found.

Keywords: Jet, impingement, blade cooling, rotational effect, PIV.

Nomenclature

C	velocity vector
D_h	jet hole hydraulic diameter
d	film cooling hole diameter
L	distance between jet and target wall
$\dot{m}_{feed,in}$	feeding channel inlet mass flow rate

$\dot{m}_{feed,out}$ feeding channel exhausted mass flow rate

$\dot{m}_{SH}$ showerhead film cooling mass flow rate

$\dot{m}_{SS}$ suction side film cooling mass flow rate

$\dot{m}_{PS}$ pressure side film cooling mass flow rate

|wall. Indeed, the accelerated stream of flow entering the jet hole, may act a blockage effect on the near web wall flow, so causing its deviation towards the channel lateral walls and the growth of secondary vorticity responsible for the onset of the commented vortex cells. These latter, are then convected downstream by the mean flow. This explanation need to be verified by additional dedicated test.

When Ro_j=0.05 cases are analysed (Figs. 7 (d-f, j-l) and Figs. 8(d-f)), an even more evident flow unbalancing is observed, but this time the velocity peak is found on the duct trailing side (y<0, PS). Indeed, rotational effects prevail over every possible source of flow non symmetry found for

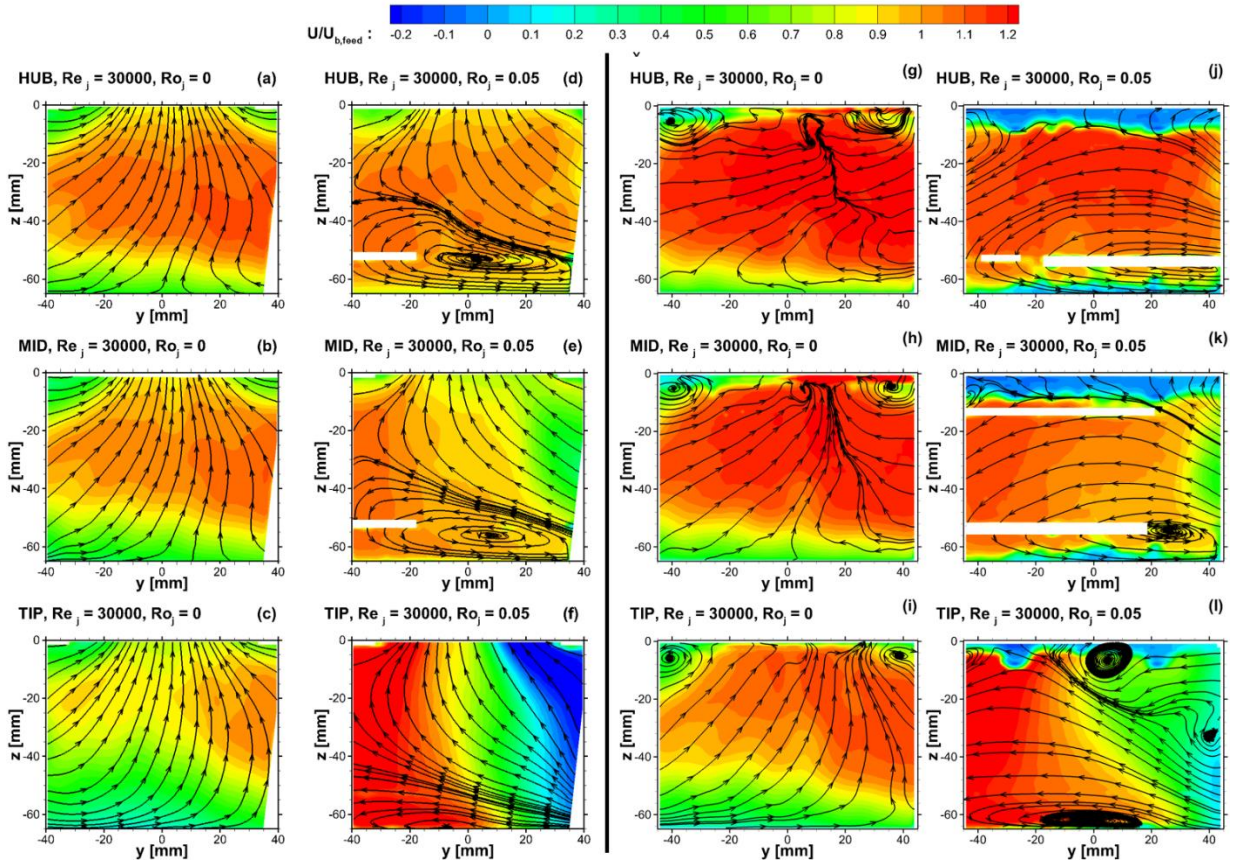

Figure 7: Feeding channel - velocity contours on planes yz1 (a-f) and yz2 (g-l), for static (odd columns) and rotating (even columns) conditions and for HUB (top line), MID (central line) and TIP (bottom line) cross flow cases.

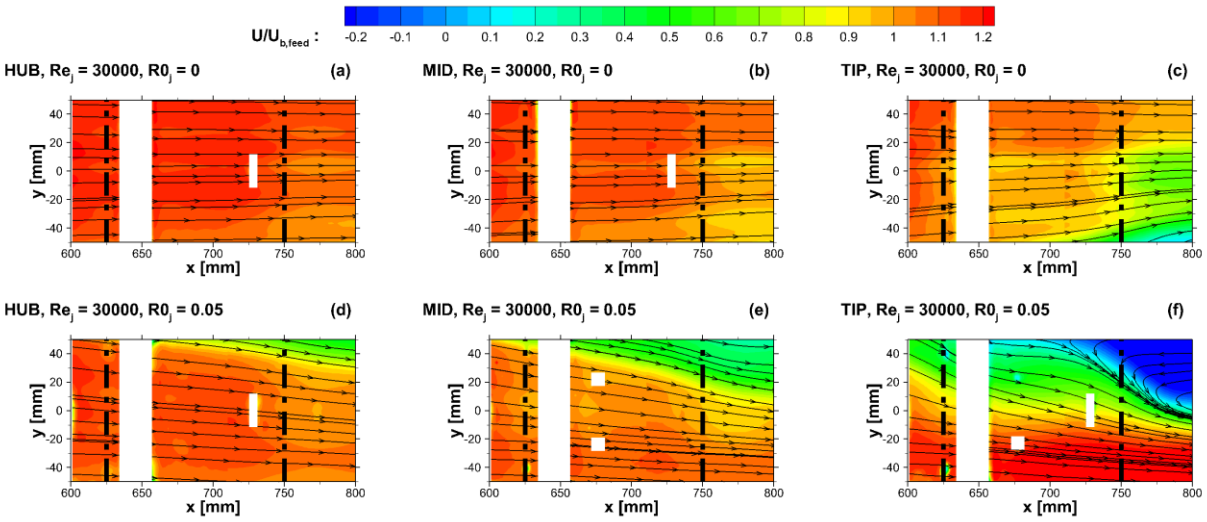

Figure 8: Feeding channel - velocity contours on plane xy for static (top line) and rotating conditions (bottom line), and at variable cross flow conditions (HUB, MID, TIP respectively in the first, second, and third column.

Ro_j=0. Again, the cross-wise velocity gradient is much stronger at the TIP where its amplitude is so high to cause velocity reversal at the duct leading side (see the blue/negative areas at y>0 in Fig. 7(f) and Fig. 8(f) for x>750). The origin of this unbalancing is strictly linked to the rotational effects that are commonly expected inside a radial flow duct in orthogonal rotation [17] and that, as previously explained, are made stronger at the TIP since the local Ro is much higher than for the HUB case. Coriolis forces are also responsible for the secondary vortical structures found in the yz planes (both 1 and 2) for Ro_j=0.05 (Figs. 7(d-f, j-l)). In particular a wide counter clockwise vortex is always found close to the bottom wall, while the opposite clockwise structure is observed close to the web-wall (z=0) only for the TIP case and in between the jet holes (Fig 7(l)). With specific reference to this position, it is also found that rotation causes the disappearance of the horseshoes vortices produced on the sides of the jet-hole for Ro_j=0 (see z>-20 for Figs. 7(g-i)). Evidently, the appearing of the secondary vorticity associated to the Coriolis vortical structures determines a different behaviour of the near web wall flow with respect to the static case. Again, the available data does not allow to draw a definitive explanation of this behaviour. However, it has to be pointed out that this local flow features does not affect the jet behaviour (as it will be seen in the next section) which is the main focus of this contribution and the more important aspect for the cooling effectiveness of the device.

In order to better visualize the 3-D flow structures that develop inside the feeding channel, a schematization is proposed in Fig. 9, representing the TIP crossflow condition in both static (a) and rotating (b) conditions.

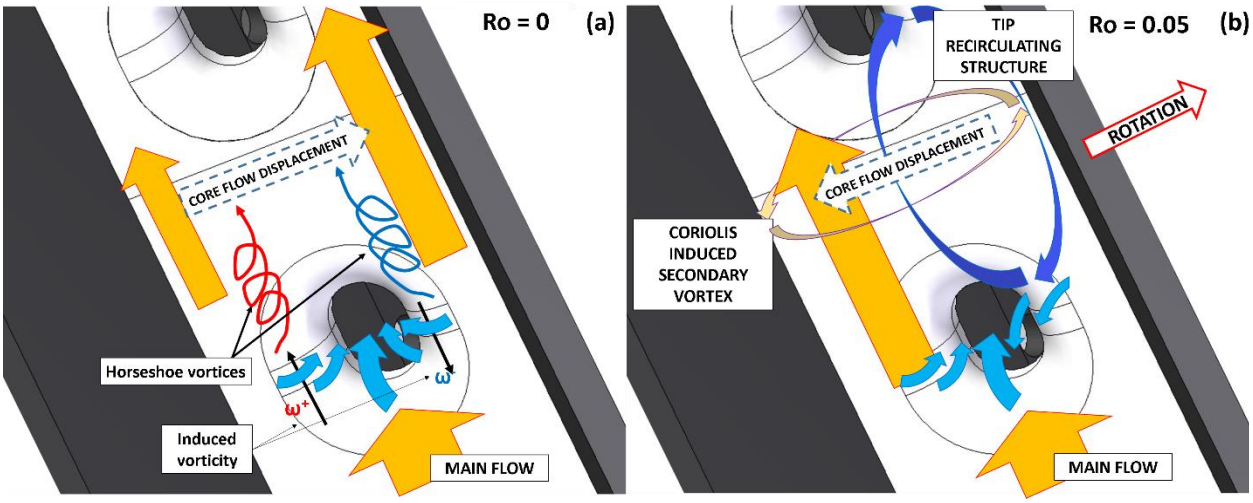

Figure 9: Feeding channel – schematization of the 3-dimensional flow structures development for the cross-flow condition TIP

3.2 Jet Flow

Figure 10 reports in plane streamtracers path and contour levels of the W velocity component for the measurements conducted inside the jet core on planes xz (frames a-f) and yz (frames g-l). The results at Ro_j=0 for HUB, MID and TIP crossflow conditions are presented in the first and third columns. The first main feature of the jet core flow is the remarkable bending towards the tip that can be appreciated by the data in the xz plane (frames a-c). As the crossflow condition is changed from HUB to TIP the bending is reduced and the jet core widens, hence lowering its velocity peak. The velocity profiles extracted at z=40.1, namely 10mm from the web wall, (solid lines in Fig. 11(a)) allow a more quantitative analysis that confirms this observation. As it can be seen, as the crossflow increases, the jet peak velocity increment is amplified. The maximum velocity in MID conditions is 10% higher than the velocity for the TIP case. A further increase in the jet velocity peak of about 20% is found if the cross flow is augmented from MID to HUB condition. Consistently with a constant flow rate through the jets imposed for every cross flow condition, the jet core reduced accordingly. These features could result in different heat transfer on the jet

target surface (i.e. the blade leading edge) as the cross flow increases, generating smaller spots of higher heat transfer.

The data on the other perpendicular plane, yz in Figs. 10(g-i) and Fig. 11(b), show a rather good flow symmetry, with lower velocity peaks found in the jet core for the TIP case in agreement with

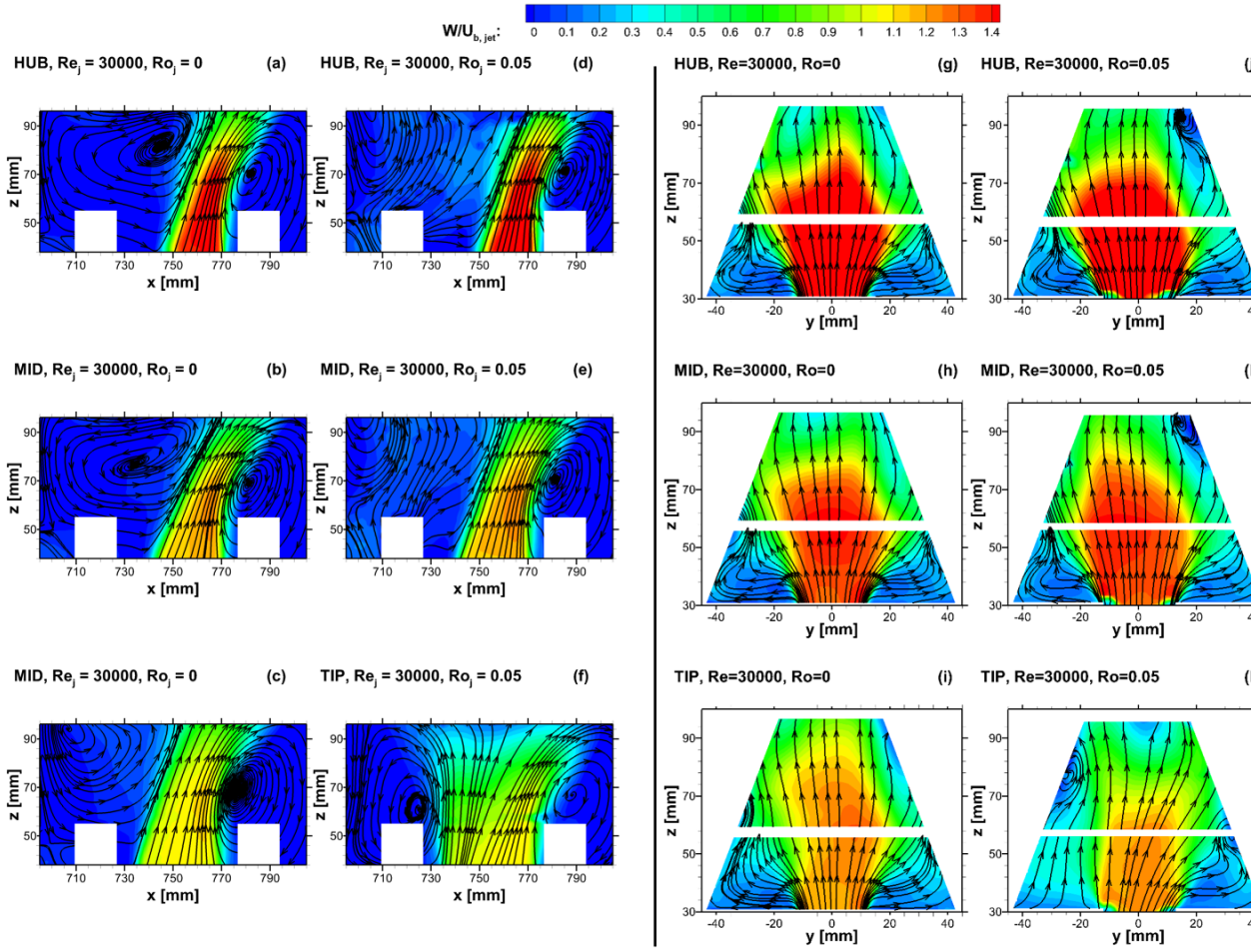

Figure 10: Impingement channel - velocity contours on planes xz (a-f) and yz (g-l), for static (odd columns) and rotating (even columns) conditions and for HUB (top line), MID (central line) and TIP (bottom line) cross flow cases.

the previous discussion. If the data at Ro_j=0.05 are considered (Figs. 10(d-f, j-l)), only marginal differences can be appreciated with respect to the static case. Indeed both the velocity distribution and the time averaged flow path depicted by the streamtracers are rather similar.

The data for Ro_j=0.05 are presented with dashed lines. All the main features of the jet, i.e. bending toward radial (x) direction that deceases from HUB to TIP and symmetrical distribution along circumferential (y) direction, are almost identical to what is observed for Ro_j=0. Therefore, it can be concluded that no significant rotation effects are able to alter the jet core velocity distribution. From a physical point of view, the main reason of this observation is that the jet is mainly aligned with the rotation axis, hence only a minor velocity component contributes to the generation of the Coriolis acceleration (ac=-2ΩxC). Moreover, as well as discussed in the open literature [18], even if small Coriolis effects are produced, their main effect is found in the low velocity areas, such as boundary layer flows or recirculating flow regions. Therefore, in the present case if remarkable rotational effects occur, they might be found far from the jet core, i.e. inside the flow volume that has not yet been investigated.

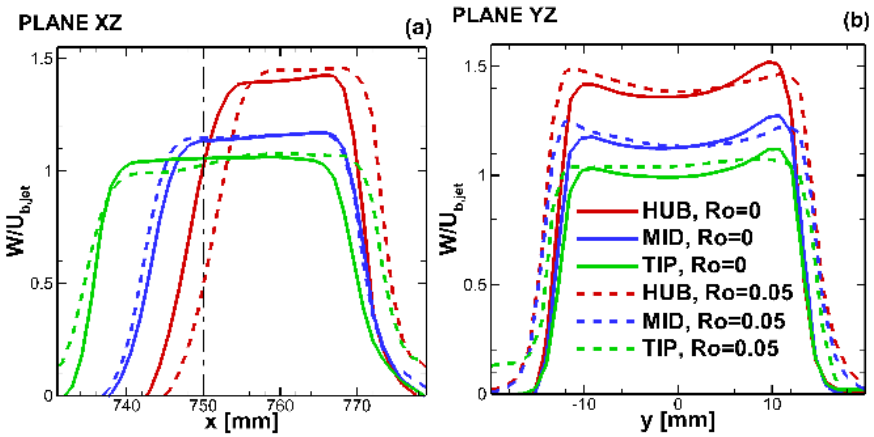

Figure 11: Jet velocity profiles extracted from plane xz at z=40.1mm (a) and yz at z= 34.1 (b).

3.3 Reynolds dependence

Reynolds number dependence has been investigated repeating every measurement for the MID zone with Re_j=10k (i.e. on every plane and both for static and rotating conditions).

In this particular geometry, the most important feature to be characterized is the jet, indeed the thermal performances mainly depend on its aerodynamics. In order to quantitatively evaluate the jet's Reynolds number dependence, in Fig. 12 the comparison between the velocity profiles from

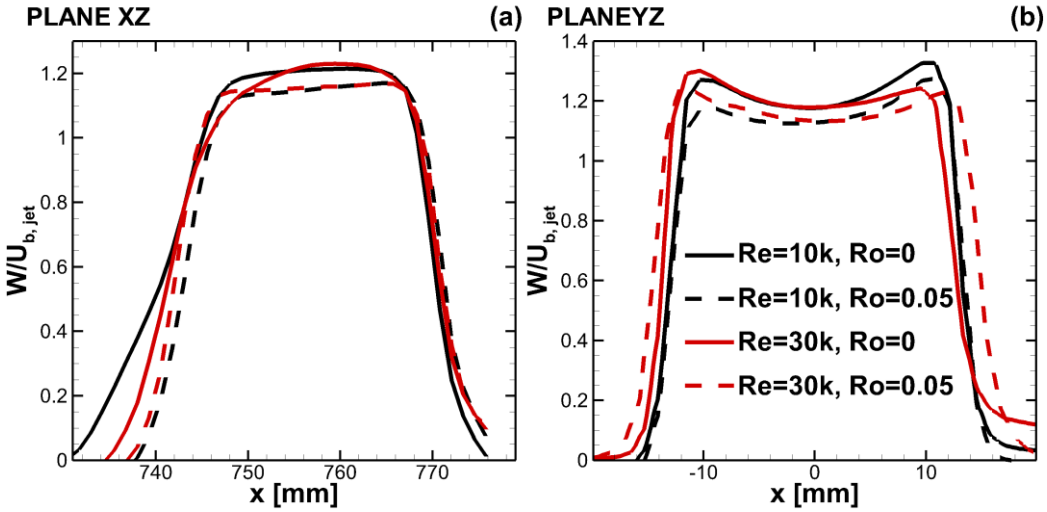

Figure 12: Jet velocity profiles extracted from plane xz at z=40.1mm (a) and yz at z= 34.1 (b) for Reynolds numbers of 30000 and 10000.

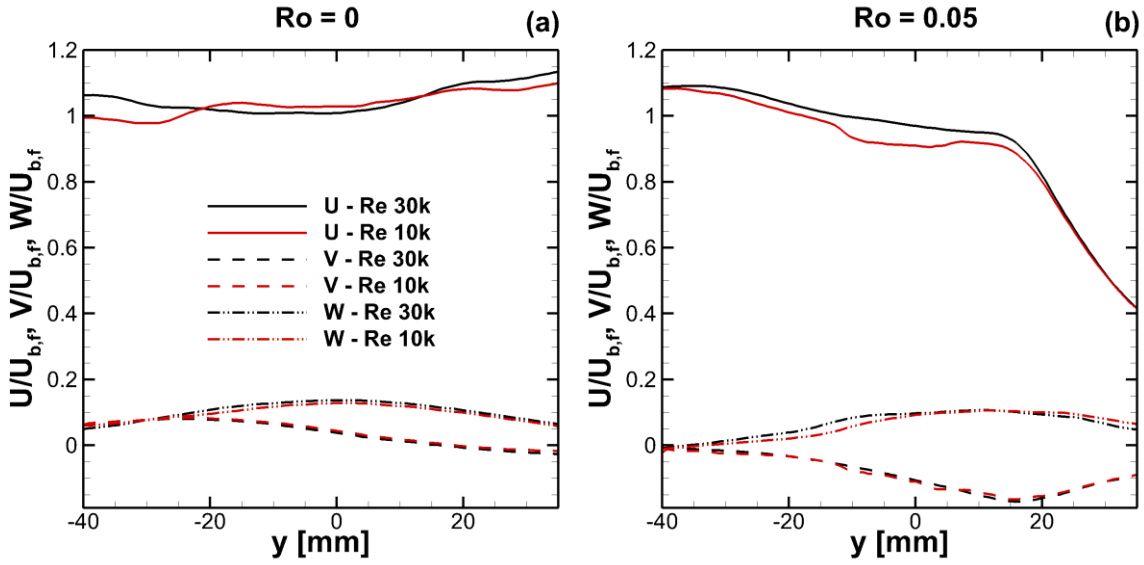

Figure 13: Feeding channel velocity profiles extracted from plane yz1 at z =-32.9 mm for Reynolds numbers of 30000 and 10000: (a) static, (b) rotating condition.

tests at Re = 30k and Re = 10k are shown. The reported data clearly show the Reynolds number variation has almost no effect on the jet flow structure, both in static and rotating conditions, at least in the investigated range.

In order to extend these conclusions (i.e. jet Re-independency in both static and rotating conditions) to the overall channel aerodynamics, the flow field in the feeding channel can be analysed with this perspective. Velocity components profiles extracted from plane yz1 are shown in Fig. 13. For both static and rotating conditions, the three velocity components (i.e. V, W in plane while U out of plane) perfectly match, showing that also in the feeding channel the flow field is Reynolds independent.

4 Conclusion

The main conclusions that can be drawn are listed in the following.

- In static conditions, the flow field inside the feeding channel is unbalanced towards the suction side. The feature is emphasized in correspondence of the jet intake.
- In rotating conditions, the behaviour is the opposite. Coriolis forces are responsible for a strong crossflow deflection toward the duct trailing side (blade pressure side) that increases in magnitude from HUB to TIP conditions. For the latter case, the unbalancing is so strong to sustain a recirculating region (negative streamwise velocity) found downstream of the central jet-hole.

Concerning the jet aerodynamic, the main features are as follows.

- The jet core is substantially bended towards the blade tip. The effect is reduced when moving from HUB to TIP conditions. In the crosswise direction, a substantial flow symmetry is found inside the jet core.
- Rotational effects do not produce any significant modification of the jet structure.

- Finally, a substantial Re independence has been found for the analysed range of flow conditions.

Further investigation will be aimed at deepening the understanding of the flow field inside the jet channel, with particular attention for the region close to the extraction holes.

Acknowledgements

This work has been supported by the Italian Ministry of University and Research (MiUR). The contribution of the ERICKA project is also acknowledged for the test section geometry.

References

[1] D.D. Luo, C.W. Leung, T.L. Chan, (2004), Forced convection and flow friction characteristics of air cooled horizontal equilateral triangular ducts with ribbed internal surfaces, Int. J. heat and Mass Transfer, vol 47, pp.5439-5450, 2004.

[2] M.E. Taslim, T. Li, S.D. Spring, (1997), Measurement of heat transfer coefficients and fiction factors in rib roughened channels simulating leading edge cavities of a modern turbine blade, J. Turbomachinery, vol. 119, pp 601-609.

[3] M. Schuller, H.M. Dreher, S.O. Neumann, B. Weigand, M. Elfert, (2010), Numerical prediction of the effect of rotation on fluid flow and heat transfer in an engine similar two pass internal cooling channel with smooth and ribbed walls, Asme paper GT2010-22870, proc. ASME Turbo Expo 2010, June 14-18, Glasgow, UK.

[4] A. Amro, B. Weigand, R. Poser, M. Schneider, (2007), An experimental investigation of the heat transfer in a ribbed triangular cooling channel, Int. J. of Thermal Science, vol. 46, pp. 491-500.

[5] N. Domaschke, J. Von Wolfersdorf, K. Semmler, (2009), Heat transfer and pressure drop measurements in a rib roughened leading edge cooling channel, Asme paper GT2009-59399, Proc. ASME Turbo Expo 2009, June 8-12, Orlando, Florida, USA.

[6] Y.H. Liu, M. Huh, J.C. Han, H.K. Moon, (2009), High rotation number effect on the heat transfer in a triangular canne with 45°, inverted 45°, and 90° ribs, Asme paperGT2009-59216, Proc. ASME Turbo Expo 2009, June 8-12, Orlando, Florida, USA.

[7] D.H. Lee, D.H. Rhee, H.H. Cho, (2006), Heat transfer measurements in a rotating equilateral triangular channel with various rib arrangements, Asme paper GT2006-90973, proc. ASME Turbo Expo 2006, may 8-11, Barcelona, Spain.

[8] Z. Liu, Z. Feng, L. Song, (2010), Numerical study of flow and heat transfer of impingement cooling on a model of turbine blade leading edge, Asme paper GT2010-23711, Proc. ASME Turbo Expo 2010, June 14-18, Glasgow, UK.

[9] J.J. Hwang, C.S. Cheng, (2001), Impingement cooling in triangular ducts using an array of side-entry wall jets, Int. J. heat and Mass Transfer, vol 44, pp. 1053-1063.

[10] M.E. Taslim, D. Bethka, (2007), Experimental and numerical impingement heat transfer in an airfoil leading edge cooling channel with crossflow, Asme paper GT2007-28212, proc. ASME Turbo Expo 2007, May 14-17, Montreal, Canada.

[11] M.E. Taslim, Y. Pan, K. Bakhtari, (2002), Experimental racetrack shaped jet impingement on roughened leading edge wall with film holes, Asme paper GT2002-30477, proc. ASME Turbo Expo 2002, June 3-6, Amsterdam, The Netherlands.

[12] M.E. taslim, A. Khanicheh, (2005), Experimental and numerical study of impingement on an airfoil leading edge with and without showerhead and gill film holes, GT2005-68037, proc. ASME Turbo Expo 2005, June 6-9, Reno-Tahoe, Nevada, USA.

[13] M.E. taslim, L. Setayeshgar, S.D. Spring, (2001), An experimental evaluation of advanced leading edge impingement cooling concepts, J. Turbomachinery, vol. 123, pp. 147-153.

[14] H.W.D. Chiang, H.L. Li, (2009), Jet impingement and forced convection cooling experimental study in rotating turbine blades, Asme paper GT2009-59795, Proc. ASME Turbo Expo 2009, June 8-12, Orlando, Florida, USA.

[15] Willert, C., (1997), Stereoscopic Digital Particle Image Velocimetry for Application in Wind Tunnel Flows, Meas. Sci. and Technol., 8, pp. 1465–1497

[16] Armellini, A., Mucignat C., Casarsa L., Giannattasio P., (2012), Flow field investigations in rotating facilities by means of stationary PIV systems, Meas. Sci. Technol. 23, p.025302 (11pp)

[17] Pascotto M., Armellini A., Mucignat C., Casarsa L., (2014), Coriolis Effects on the Flow Field Inside a Rotating Triangular Channel for Leading Edge Cooling, ASME J. Turbomach., 136(3), p.031019

[18] Johnston J. P., Halleen R. P., Lezius D. K., (1972), Effects of spanwise rotation on the structure of two-dimensional fully developed turbulent channel flow, J. Fluid Mech. 56, pp. 533–557